# Improving the UWB Pulseshaper Design Using Non-Constant Upper Bounds in Semidefinite Programming

Christian R. Berger, *Student Member, IEEE,* Michael Eisenacher, *Student Member, IEEE,*
Shengli Zhou, *Member, IEEE,* and Friedrich Jondral, *Member, IEEE*

*Abstract*— A critical obstacle for ultra-wideband (UWB) communications is conformity to restrictions set on the allowed interference to other wireless devices. To this end UWB signals have to comply with stringent constraints on their emitted power, defined by the FCC spectral mask. Different UWB pulseshaper designs have been studied to meet the spectral mask, out of which an approach based on digital FIR filter design via semidefinite programming has stood out. However, so far this approach has assumed an ideal basic analog pulse to use piece-wise constant constraints for the digital filter design. Since any practical analog pulse does not have a flat spectrum, using piece-wise constant constraints leads to considerable power loss. Avoiding such a loss has motivated us to implement the exact constraints through non-constant piece-wise continuous bounds. Relative to the design assuming an ideal basic analog pulse, our design examples show that the transmission power can be enhanced considerably while obeying the spectral mask. Such an improvement comes with no extra cost of implementation complexity.

*Index Terms*— Linear matrix inequalities, pulseshaper design, semidefinite programming, spectral mask, ultra-wideband.

## I. INTRODUCTION

**U**LTRA-wideband (UWB) transmission is a fast emerging technology with unique properties and has been a subject of enormous research and development efforts in recent years. It is a promising approach for high-speed short-range wireless radio links, very precise localization and ranging, and ground penetrating radar [1], [2], [3]. One target application is the Wireless Personal Area Network (WPAN) where the long-term goal is the abolition of all data wires [4].

Although there are several definitions for UWB, the Federal Communications Commission (FCC) published a widely accepted definition that characterizes UWB only by its bandwidth, independent of the employed modulation scheme [5]: A

UWB signal must either occupy an absolute 10 dB bandwidth of 500 MHz or a relative bandwidth of 20% with respect to the center frequency. Since such large unoccupied bandwidths do not exist, UWB has to work as an overlay system that re-occupies frequency bands that are already used by other radio systems. Coexistence can be achieved because UWB spreads its signal energy over a very large bandwidth which results in an extremely low power spectral density (PSD). Due to this very low PSD, UWB signals are hidden under the background noise and therefore do not cause noteworthy interference to other narrowband systems (narrowband compared to UWB).

The only authority which already admits UWB devices is the FCC [5]. The main restriction is a spectral mask, which is piece-wise constant as depicted in Fig. 1. For communication handhelds the maximum PSD in the main frequency band between 3.1 and 10.6 GHz is -41.3 dBm/MHz. This limits the range of UWB devices to about 10 m for high data rates. Thus, *one of the fundamental challenges is the maximization of the transmitted power while complying with the spectral mask.* If the spectral properties are not optimized, the output power has to be lowered to fulfill the mask requirements in every frequency band.

Since the ultra-short pulses used are generated with analog components, e.g., the Gaussian Monocycle as depicted in Fig. 1, their spectral shape is not easy to design. Replacing the analog pulses with digital designs is prohibited by the huge bandwidth and the resulting sampling rates. Using an FIR prefilter before the analog pulse generators, the spectral shape can be controlled, but due to the particular problem formulation, designing the FIR filter coefficients to maximize the resultant transmit power is not trivial. Traditional FIR design algorithms like the Parks-McClellan algorithm [6] have been used to approximate the FCC spectral mask [7], but the reduction to linear-phase filters and an equi-ripple design does not lead to an optimal solution in the sense of maximizing the transmit power.

To find the optimal FIR filter coefficients, we need to maximize the transmit power, while strictly enforcing the FCC spectral mask. This optimum formulation can be implemented via FIR filter design using semidefinite programming [8], [9], which is a type of convex optimization [10]. Numerical implementation can only handle a finite number of constraints, therefore either the constraints were approximated with a finite
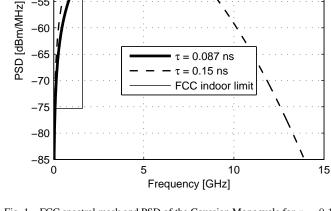
Fig. 1. FCC spectral mask and PSD of the Gaussian Monocycle for $\tau = 0.15$ ns and $\tau = 0.087$ ns

set of samples or the problem was cast into the linear matrix inequalities (LMI) framework [9]. The first approach is an obvious approximation of the truly optimal solution, while the second so far has only been used in conjunction with assuming an ideal basic analog pulse (completely constant PSD), leading to piece-wise constant constraints [11].

We are motivated to address the optimal pulseshaper design in the semidefinite programming framework. To avoid the power loss due to the piece-wise constant constraints, we use non-constant piece-wise continuous bounds that suit the optimal problem formulation, without having to use either of the aforementioned simplifications. We use a modified Fourier series expansion using non-orthogonal basis functions to approximate an arbitrary constraint. This way we can find the (near-)optimal solution for arbitrary basic analog pulses, while strictly enforcing the FCC spectral mask. We will give detailed design examples, that show considerable improvement on the transmit power relative to that of suboptimal approaches.

The rest of the paper is as follows. In Section II we will go over the standard signal model of impulse radio and describe the challenges of the pulseshaper design problem. In Section III, we will reiterate some background of the LMI formulation for FIR filter design and show how we implement non-constant bounds. Design examples will be presented in Section IV and last we will conclude in Section V.

We want to use the following notation. Bold lower and upper case letters refer to vectors and matrices, respectively. The matrix $\mathbf{I}_k$ will be the identity matrix of $k \times k$, and $\mathbf{0}_{n \times k}$ is the matrix of all zeros, with dimension $n \times k$. The superscript "$T$" denotes the transpose, "$H$" denotes the Hermitian, i.e., the complex conjugate transpose. The operator $\text{vec}(\cdot)$ applied on matrices will be a stacked vector of all matrix elements, column by column, and the "$*$" operator will denote linear convolution. We use $\mathbb{R}$ and $\mathbb{C}$ to denote the sets of real and complex numbers respectively.

## II. SIGNAL MODEL AND PULSESHAPING PROBLEM

### A. Signal Model

Our signal model will be impulse radio (IR) with time hopping (TH) and binary pulse amplitude modulation (PAM). Ultra-short pulses are the building block of this transmission scheme; the basic pulse on the channel is $p(t)$, e.g., the Gaussian Monocycle [12], with power $\int p^2(t)\,dt = \varepsilon$. One pulse is sent during each frame duration $T_f$. Each data symbol consists of $N_f$ pulses, resulting in a total symbol length $T_s = N_f T_f$. The signal model can be expressed as:

$$u(t) = \sum_k b_k \frac{1}{\sqrt{N_f \varepsilon}} \sum_{l=0}^{N_f - 1} p(t - lT_f - kT_s - c_l T_c), \quad (1)$$

where $b_k$ are the PAM symbols $\{-1, 1\}$ for each bit, $T_c$ is the chip period and $c_l$ are the user-specific TH codes, with $c_l T_c < T_f, \forall l$.

The PSD can be calculated in a standard fashion as [13]:

$$\Phi_{uu}(f) = \frac{1}{T_s N_f \varepsilon} |P(f)|^2 \left| \sum_{l=0}^{N_f - 1} e^{j2\pi(-lT_f - c_l T_c)f} \right|^2. \quad (2)$$

When assuming the TH code $c_l$ to be integer-valued, independent and uniformly distributed, $\Phi_{uu}(f)$ can be approximated as [14], [15]:

$$\Phi_{uu}(f) \approx \frac{1}{T_s \varepsilon} |P(f)|^2. \quad (3)$$

Thus, the PSD of the basic pulse $p(t)$ is crucial to the PSD of the complete UWB signal. Therefore, it is necessary to select a pulse with optimal spectral properties.

### B. Pulseshaping Problem

The basic pulses $p(t)$ used in UWB systems are created with analog RF components. Therefore, designing the pulse to comply with some specific demands like the FCC spectral mask is rather difficult (see Fig. 1). Basically only the pulse duration and amplitude can be controlled which correspond to the bandwidth and power in the PSD respectively. Different digitally created pulse shapes have been suggested [16], whereby those pulses have to be generated of digital samples. Since the pulses need bandwidths of several GHz, sampling nanosecond length pulses is highly demanding.

Using transmit filters to adapt to spectral constraints is also difficult to implement, since analog filters with an enormous bandwidth would have to be used. Instead, using an FIR filter like approach [7], [11], each basic pulse is repeated $N$ times with arbitrary amplitudes, created by the pulse generators used already for modulation. This is equivalent to prefiltering the signal before using the basic pulse as a transmit filter:

$$u(t) = \sum_k b_k \frac{1}{\sqrt{N_f \varepsilon}} \sum_{l=0}^{N_f - 1} \delta(t - lT_f - kT_s - c_l T_c) * p(t). \quad (4)$$

Now let $q(t)$ denote the analog pulses created by the usual pulse generators which can be chosen based on hardware

constraints. With prefiltering by $w_n$, which will be design parameters, the overall pulse $p(t)$ becomes

$$p(t) = \sum_{n=0}^{N-1} w_n q(t - nT) = w(t) * q(t) \qquad (5)$$

whereby $w(t) = \sum_{n=0}^{N-1} w_n \delta(t - nT)$. The PSD is accordingly

$$|P(f)|^2 = \Phi_{ww}(f) |Q(f)|^2. \qquad (6)$$

Let $S(f)$ denote the FCC spectral mask. The pulseshaping problem can now be formulated as

$$\max_{w_n} \int |P(f)|^2 \, df \quad \text{subject to } |P(f)|^2 \leq S(f), \, \forall f \qquad (7)$$

i.e., maximizing the transmit power while adhering to all spectral constraints. To solve this non-linear optimization problem is not trivial. We will next look at some existing approaches.

### C. Existing Approaches

Existing approaches are based on FIR filter design, e.g., the Parks McClellan algorithm can be used to optimize the set of $w_n$ [7]. Even though these approaches can deliver good results, optimality is not guaranteed, since the algorithm depends on equi-ripple design and does not directly maximize the transmit energy.

The prominent approach is to employ FIR filter design via semidefinite programming. To use this approach the problem formulation is changed to a linear problem as follows. Due to optimizing over the $w_n$, we only influence $\Phi_{ww}(f)$, which can be calculated as

$$\Phi_{ww}(f) = \left| \sum_{n=0}^{N-1} w_n e^{j2\pi nTf} \right|^2 = \sum_{n=-N+1}^{N-1} r_n e^{j2\pi nTf} \quad (8)$$

with $r_{|n|} = \sum_{k=0}^{N-1-n} w_k w_{k+n}$ being the non-periodic autocorrelation sequence of the $w_n$. Assuming real $w_n$, we can further simplify it to

$$\Phi_{ww}(f) = r_0 + 2 \sum_{n=1}^{N-1} r_n \cos(2\pi nTf) = \mathbf{r}^T \boldsymbol{\psi}_N(f) \, (9)$$

where we define the vectors

$$\mathbf{r} = \begin{bmatrix} r_0 \\ \vdots \\ r_{N-1} \end{bmatrix}, \; \boldsymbol{\psi}_N(f) = 2 \begin{bmatrix} \frac{1}{2} \\ \cos[2\pi fT] \\ \vdots \\ \cos[2\pi(N-1)fT] \end{bmatrix}. \tag{10}$$

The PSD $\Phi_{ww}(f)$ will be periodic in the additional design parameter $1/T$, therefore we choose the frequency range $\mathcal{F}_p$ to be $[0, 1/2T]$ since this is the interval in which we will be able to affect the design. Outside this interval we will assume $|Q(f)|^2$ to be small enough to attenuate the periodic repetitions of $\Phi_{ww}(f)$. Accordingly $T$ and $q(t)$ will have to be chosen jointly.
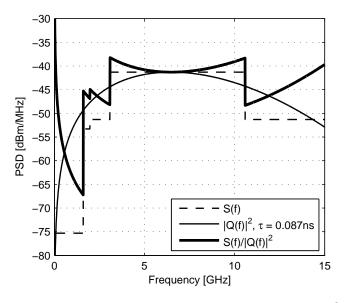


Fig. 2. To formulate completely linear constraints, we use $S(f)/|Q(f)|^2$ as upper bound.

Since the problem formulation in (7) is non-linear in $w_n$, to find a linear problem we will reformulate it with respect to $\mathbf{r}$

$$\int_{\mathcal{F}_p} |P(f)|^2 df = \int_{\mathcal{F}_p} \mathbf{r}^T \boldsymbol{\psi}_N(f) |Q(f)|^2 \, df = \mathbf{r}^T \mathbf{c}, \quad (11)$$

where $\mathbf{c} = \int_{\mathcal{F}_p} \boldsymbol{\psi}_N(f) |Q(f)|^2 \, df$ is the projection of $|Q(f)|^2$ onto the basis functions.

Under the additional constraint that $r_n$ are a valid autocorrelation sequence, which is equivalent to $\Phi_{ww}(f) \geq 0, \, \forall f$, we can write the linear optimization problem as,

$$\max_{\mathbf{r}} \mathbf{r}^T \mathbf{c} \quad \text{subject to } 0 \leq \mathbf{r}^T \boldsymbol{\psi}_N(f) \leq \frac{S(f)}{|Q(f)|^2}, \; f \in \mathcal{F}_P. \tag{12}$$

This leads to a new set of constraints, e.g., see Fig. 2 for a Gaussian monocycle with $\tau = 0.087$ ns. As stated before, this formulation fits a typical FIR filter design problem, specifying upper and lower bounds on the PSD. Since we are indifferent as to the gain in individual parts of the spectrum, the lower bound is not very demanding, but instead we maximize the total energy within the frequency range of interest.

Since the optimization problem in (12) has an infinite number of linear constraints, one approach is based on sampling the constraints and introduces an additional relaxation to ensure compliance for all $f \in \mathcal{F}_P$.

The approach we want to focus on is based on replacing the infinitely many constraints with a finite size linear matrix equation and limiting some of the optimization variables as elements of semidefinite matrices [11]. This can be achieved using a linear matrix inequality (LMI) formulation derived for FIR filter design [9], but so far has only been used in conjunction with approximating the basic analog pulse $|Q(f)|^2$ as constant within $\mathcal{F}_P$. The formulation does not depend on an equi-ripple design and achieves globally optimal solutions via convex optimization.

The approximation of a constant basic analog pulse PSD leads to a simplified problem formulation within the LMI framework [9]. Assuming a constant PSD basic pulse, one could use the following six constraints to follow the piece-wise constant spectral mask $S(f)$:

$$
\begin{aligned}
\Phi_{ww}(f) &\geq 0, \quad f \in \mathcal{F}_P \\
\Phi_{ww}(f) &\leq -75.3 \text{ dB}, \ f \in [0, 1.6] \text{ GHz} \\
\Phi_{ww}(f) &\leq -53.3 \text{ dB}, \ f \in [0, 1.9] \text{ GHz} \\
\Phi_{ww}(f) &\leq -51.3 \text{ dB}, \ f \in [0, 3.1] \text{ GHz} \\
\Phi_{ww}(f) &\leq -41.3 \text{ dB}, \ f \in \mathcal{F}_P \\
\Phi_{ww}(f) &\leq -51.3 \text{ dB}, \ f \in [10.6, 1/2T] \text{ GHz}.
\end{aligned} \tag{13}
$$

The filter design with the piece-wise constant constraints on $\Phi_{ww}(f)$ is solved in [11].

Even though there are pulses which have a somewhat constant PSD in the spectrum of interest (see Fig. 1), this does not hold for arbitrary analog pulses, e.g., dictated by hardware constraints. We will later quantify the losses due to this simplification in the design, but in any case this does not qualify as an optimal solution.

### D. Proposed Solution

To achieve an optimal solution, arbitrary constraints on the PSD will have to be implemented in the LMI formulation. This way we will be able to provide optimal solutions for arbitrary analog pulses. Naturally some pulses will have better performance than others; and it seems likely that pulses close to the constant PSD approximation will perform the best. In any case, for any given analog pulse we will be able to supply an optimal set of coefficients $w_n$.

The LMI formulation in [9] provides piece-wise constant, but also piece-wise trigonometric polynomial constraints. We will use the latter to implement piece-wise continuous constraint functions $\Gamma(f)$, which enables us to enforce any constraints, as long as they have a finite number of discontinuities. As will be clear later on, one set of new constraints would be:

$$
\begin{aligned}
\Phi_{ww}(f) &\geq 0, \quad f \in \mathcal{F}_P \\
\Phi_{ww}(f) &\leq \Gamma_1(f), \ f \in [0, 1.61] \text{ GHz} \\
\Phi_{ww}(f) &\leq \Gamma_2(f), \ f \in [0, 1.99] \text{ GHz} \\
\Phi_{ww}(f) &\leq \Gamma_3(f), \ f \in [0, 3.1] \text{ GHz} \\
\Phi_{ww}(f) &\leq \Gamma_4(f), \ f \in \mathcal{F}_P \\
\Phi_{ww}(f) &\leq \Gamma_5(f), \ f \in [10.6, 1/2T] \text{ GHz}
\end{aligned} \tag{14}
$$

where $\Gamma_i(f)$ are non-constant. See e.g., Fig. 5 for the constraints due to a Gaussian Monocycle basic pulse with $\tau = 0.087$ ns. The questions we address in this paper are:

1) *How can we implement arbitrary non-constant bounds as piece-wise trigonometric polynomials provided by the LMI framework?*
2) *What upper bounds can we use and which ones lead to the best performance?*

## III. THE DESIGN PROCEDURE WITH NON-CONSTANT UPPER BOUNDS

### A. Review of Linear Matrix Inequalities

Linear matrix inequalities (LMI) are used in FIR filter design to convert spectral constraints into linear constraints on elements of positive semidefinite matrices. This way, the FIR filter design problem can be effectively solved via semidefinite programming.

Semidefinite programming is a form of convex optimization [17], [10], which adds convex constraints to a linear formulation. This can be solved efficiently and globally optimally using interior-point methods, e.g. [18]. By defining part of the optimization variables as elements of positive semidefinite matrices, they are restricted to a convex space. In this way many non-linear problems, e.g., quadratic optimization, can be reduced to a linear problem with convex constraints (see [17], [10] for more details).

To give an example of how spectral constraints can be converted into an LMI, we will revisit the origin of semidefinite programming in FIR filter design, which is the Positive-Real lemma for FIR systems [8] later simplified in [19], [20] to the following form:

**Lemma 1**

$$
\Phi_{ww}(f) = \sum_{n=-N+1}^{N-1} r_n e^{j2\pi nTf} \geq 0
$$
$$
\Leftrightarrow \exists \mathbf{X} \in \mathbb{C}^{N \times N} \mid \mathbf{X} \succeq 0 \tag{15}
$$
$$
\sum_{i=0}^{N-1-k} [\mathbf{X}]_{i,i+k} = r_k, \ k = 0, \ldots, N-1
$$

where $\mathbf{X} \succeq 0$ stands for the positive semidefinite property.

We see that the spectral constraint on the left of (15) are converted to linear constraints on the elements of a positive semidefinite matrix. (We also provide a short and simple proof of (15) in the Appendix).

In the following we will briefly reiterate the LMI results from [9], as needed for our problem formulation. We use a simplified and applied version of the main result in [9, *Theorem* 3], as suggested in the FIR filter design example in [9].

Let $\Gamma(f)$ denote a sum of trigonometric functions, as in a Fourier series expansion,

$$
\Gamma(f) = \sum_{-N+1}^{N-1} \gamma_n e^{j2\pi nfT} = \boldsymbol{\gamma}^T \boldsymbol{\psi}_N(f), \tag{16}
$$

where $\boldsymbol{\gamma} := [\gamma_{-N+1}, \ldots, \gamma_{N-1}]^T$. To implement trigonometric polynomial bounds of the form

$$
\Phi_{ww}(f) \leq \Gamma(f), \quad f \in \left[ \frac{\alpha}{T}, \frac{1-\alpha}{T} \right], \tag{17}
$$

the following formulation can be used:

$$r_k = \begin{cases} \gamma_k - (g_0 + d_0 h_0 + 2d_1 h_1), & k = 0 \\ \gamma_k - (g_k + d_{-1}h_{k+1} + d_0 h_k + d_1 h_{k-1}), & 1 \le k \le N-3 \\ \gamma_k - (g_{N-2} + d_0 h_{N-2} + d_1 h_{N-3}), & k = N-2 \\ \gamma_k - (g_{N-1} + d_1 h_{N-2}), & k = N-1 \end{cases} \qquad (19)$$

**Lemma 2**

$$\sum_{n=-N+1}^{N-1} r_n e^{j2\pi nfT} \le \Gamma(f), \ f \in \left[\frac{\alpha}{T}, \frac{1-\alpha}{T}\right]$$

$$\Leftrightarrow \exists \mathbf{X} \in \mathbb{R}^{N \times N}, \mathbf{Z} \in \mathbb{R}^{(N-1) \times (N-1)} \mid \mathbf{X}, \mathbf{Z} \succeq 0, \qquad (18)$$

$$\sum_{i=0}^{N-1-k} [\mathbf{X}]_{i,i+k} = g_k, \quad \sum_{i=0}^{N-2-k} [\mathbf{Z}]_{i,i+k} = h_k$$

*where the $r_n$ are in the linear relationship to the $g_n$, $h_n$ and $\gamma_n$ given in (19)and the $d_n$ are chosen such that*

$$\sum_{n=-1}^{1} d_n e^{j2\pi nTf} = d_0 + 2d_1 \cos(2\pi nTf) \ge 0, \qquad (20)$$

*for all $f \in \left[\frac{\alpha}{T}, \frac{1-\alpha}{T}\right]$, e.g., $d_0 = 2\cos\alpha$ and $d_1 = d_{-1} = -1$.*

For a complementary formulation where the bound in (18) is defined on $f \in \left[0, \frac{\alpha}{T}\right] \cup \left[\frac{1-\alpha}{T}, \frac{1}{T}\right]$, we can interchange the positive and negative intervals in (20) by using $\tilde{d}_n = -d_n$.

*B. Implementing Linear Matrix Inequalities for Non-Ideal Analog Pulses*

To implement non-constant constraints, we will use trigonometric polynomials. It might seem possible to use only one constraint to represent the whole spectral mask. Although we can choose the function $\Gamma(f)$ as the Fourier series expansion of any spectral mask $S(f)$ which might serve as a constraint, this approximation has well known limits. Especially at discontinuities, which lead to the Gibbs Phenomenon, this approximation can lead to problems. More specifically, if the Gibbs Phenomenon leads to any negative value in an upper bound, this would make no solution possible, since $\Phi_{ww}(f) \ge 0 \ \forall f$ is an implicit constraint when working with the autocorrelation coefficients $r_n$.

We propose to cut the constraints into "well-behaved" sections, which will then serve as piece-wise continuous upper bounds. However, when approximating only part of $S(f)/|Q(f)|^2$ the Fourier series expansion cannot be used because the cosine functions are *not orthogonal* on an arbitrary interval $[\alpha, \beta]$. Instead, minimizing the squared error for the base function system $\boldsymbol{\psi}_N(f)$ on some particular interval,

$$\min_{\boldsymbol{\gamma}} \int_{\alpha}^{\beta} \left| S(f) - \boldsymbol{\gamma}_n^T \boldsymbol{\psi}_N(f) \right|^2 df, \qquad (21)$$

leads to solving a linear equation system. This is equivalent to orthogonalizing the autocorrelation matrix of the base functions on this interval and comes out to:

$$\boldsymbol{\gamma}^H \int_{\alpha}^{\beta} \boldsymbol{\psi}_N(f) \boldsymbol{\psi}_N(f)^T df = \int_{\alpha}^{\beta} S(f) \boldsymbol{\psi}_N(f)^T df. \qquad (22)$$

This way, very good approximations of any piece-wise continuous function serving as an upper bound can be achieved.

As an example see Fig. 3, where the center section of $S(f)/|Q(f)|^2$ for $\tau = 0.087$ ns is approximated.

To solve the optimal problem formulation in (12), we will use six LMIs, as suggested in (14). This will make it possible to enforce the non-constant constraints within the semidefinite programming framework.

We summarize the steps in finding the solution to (12) with constraints in (14) as follows:

1) Choose the basic pulse $q(t)$ and design parameter $T$, fix the FIR filter length $N$.
2) Define a positive definite matrix $\mathbf{X}_0$ for the PSD assumption. This leads to the following linear formulation,

$$\begin{bmatrix} \mathbf{I}_N & -\mathbf{F} \end{bmatrix} \begin{bmatrix} \mathbf{r} \\ \text{vec}(\mathbf{X}_0) \end{bmatrix} = \mathbf{0}_{N \times 1} \qquad (23)$$

where the matrix $\mathbf{F}$ is of dimension $N \times N^2$ and characterizes the linear relationships given in (15).
3) Divide the constraints into piece-wise continuous sections $i$, $i = 1, \ldots, I$; there will be one set of constraints extending from the start of $\mathcal{F}_p$ and one from extending from the end. For each bounding functions $\Gamma_i(f)$, determine the $\boldsymbol{\gamma}_i$ via (22).
4) Define two positive semidefinite matrices $\mathbf{X}_i$ and $\mathbf{Z}_i$ for each piece-wise continuous constraint. Construct the linear relationships as matrix equations from (19)

$$\begin{bmatrix} \mathbf{I}_N & \mathbf{F} & \mathbf{G}(\alpha) \end{bmatrix} \begin{bmatrix} \mathbf{r} \\ \text{vec}(\mathbf{X}_i) \\ \text{vec}(\mathbf{Z}_i) \end{bmatrix} = \boldsymbol{\gamma}_i \qquad (24)$$
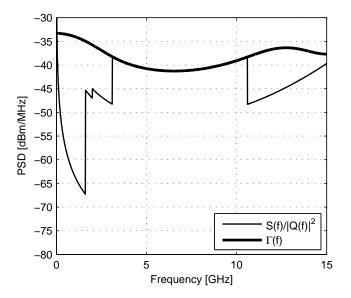


Fig. 3. Approximation of $S(f)/|Q(f)|^2$ in the center interval through an upper bound function $\Gamma(f)$.

where $\mathbf{F}$ is the same as above and $\mathbf{G}$ is of dimensions $N \times (N-1)^2$ and depends on $\alpha$ via the $d_n$.

5) We finally need to solve a standard linear problem

$$\max_{\mathbf{x}} \tilde{\mathbf{c}}^T \mathbf{x} \quad \text{subject to} \quad \mathbf{A}\mathbf{x} = \mathbf{b} \qquad (25)$$

with convex constraints on the optimization variables:

$$\mathbf{x} \in \mathbb{R}^N \times \text{vec}(\mathbf{X}_0) \times \text{vec}(\mathbf{X}_1) \times \text{vec}(\mathbf{Z}_1) \times \ldots$$
$$\times \text{vec}(\mathbf{X}_I) \times \text{vec}(\mathbf{Z}_I). \quad (26)$$

The optimization variables $\mathbf{x}$ therefore consist of $\mathbf{r} \in \mathbb{R}^N$ and the stacked (real) elements of all matrices $\mathbf{X}_i$, $\mathbf{Z}_i$. The vector $\tilde{\mathbf{c}}$ is $\mathbf{c}$ appended with zeros, and $\mathbf{A}$, $\mathbf{b}$ include the PSD assumption from (23) and $I$ linear constraints of type (24). We use the optimization package in [18], i.e., SeDuMi 1.1, to solve this optimization problem.

## IV. DESIGN EXAMPLES

To compare different designs, we will use the the effective power usage ratio $\eta$ as the figure of merit, which is defined as the ratio of achieved signal power to the maximum power possible limited by the FCC spectral mask $S(f)$ within the frequency interval of interest $\mathcal{F}_p$:

$$\eta = \frac{\int_{\mathcal{F}_p} |P(f)|^2 \, df}{\int_{\mathcal{F}_p} S(f) \, df}. \qquad (27)$$

Clearly $0 < \eta \le 1$. The larger $\eta$, the better the performance.

For all design examples we will use $T = 0.0333$ ns and accordingly $\mathcal{F}_p = [0, 15]$ GHz, the Gaussian Monocycle $q(t)$ has the following PSD

$$|Q(f)|^2 \propto f^2 \exp\left[-\pi(\tau f)^2\right] \qquad (28)$$

where we change the parameter $\tau$ for two different design examples. We divide the FCC mask $S(f)$ into five sections as described in (13) and (14) either using the constant basic pulse PSD assumption or the new non-constant bounds.

### A. Losses Due to Assuming the Basic Pulse Having a Constant PSD

First we will assess the losses of using the piece-wise constant bounds in (13). Assuming the pulse PSD (28) to be flat over an area of easily 10 GHz is a very strong simplification, even when using a pulse chosen to be as constant as possible at the frequencies of interest (see $|Q(f)|^2$ for $\tau = 0.087$ ns in Fig. 1). Nevertheless, assuming an ideal pulse with flat PSD, we find $\Phi_{ww}(f)$ that leads to $\eta_{\text{old}}^i$ in Table I. The actual PSD of the pulse $|P(f)|^2 = \Phi_{ww}(f)|Q(f)|^2$ leads to $\eta_{\text{old}}$ in Table I. Hence, the real pulse $|Q(f)|^2$ leads to a considerable loss of $10 \log_{10} \eta_{\text{old}}^i / \eta_{\text{old}}$ dB, as shown in Table I. These losses are most noticeable when $\eta$ approaches unity for high lengths of $N$, but they will be much higher if the basic pulse $q(t)$ cannot be freely chosen, e.g., due to hardware constraints, because any other pulse would be even further from the constant spectrum assumption. We will give a more drastic example later.

So a first evaluation of the simplification of constant basic pulse PSD shows losses which increase with the optimality of the solution. This is counter productive to the goal of an optimal solution.
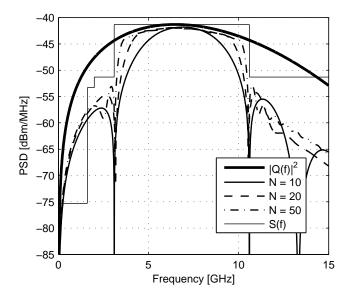


Fig. 4.   Losses due to non-ideal pulse of $\tau = 0.087$ ns

| N | 10 | 20 | 50 |
|---|---|---|---|
| $\eta_{\text{old}}^i$ ideal pulse $\tau = 0$ ns | 0.6342 -1.978 dB | 0.8209 -0.857 dB | 0.9299 -0.321 dB |
| $\eta_{\text{old}}$ real pulse $\tau = 0.087$ ns | 0.5350 -2.716 dB | 0.6694 -1.743 dB | 0.7374 -1.323 dB |
| losses due to real pulse | -18.5% 0.738 dB | -22.6% 0.8857 dB | -26.0% 1.002 dB |

TABLE I

PERFORMANCE ASSUMING AN IDEAL PULSE AND LOSSES DUE TO REAL PULSE PSD

### B. The Proposed Design With The Basic Pulse Having $\tau = 0.087$ ns

Even when split up into piecewise-continuous intervals, to get good approximations, the needed upper bounds cannot have a too high derivative, since this can lead to difficulties with the Fourier series expansion for small $N$. When dividing by the PSD of the Gaussian monocycle, the derivative can become very high in $\Gamma_1(f)$ and $\Gamma_5(f)$, c.f., Fig. 2 and (14).

To avoid poor approximations, $S(f)/|Q(f)|^2$ has to be limited. This is most easily accomplished by cutting off values, e.g., when values in an interval reach a certain multiple of the smallest value. In Fig. 5 values were cut off when 6 dB above the smallest value of their interval.

Fig. 6 shows a design example of $\Phi_{ww}(f)$. It can be seen how $\Phi_{ww}(f)$ approaches $S(f)/|Q(f)|^2$ very well (results are plotted for different values of $N$). $\Phi_{ww}(f)$ would actually be above $S(f)$ before being multiplied with $|Q(f)|^2$, but this just shows the extent the allowed energy radiation had not been exploited by assuming the Gaussian monocycle to be constant.

The exact PSD of the waveform $|P(f)|^2$ is obtained after multiplication with $|Q(f)|^2$ (see Fig. 7). Due to using the extended definition of the upper bounds, results after multiplication fit the FCC spectral mask very well. For larger pulse train length $N$, results for $\eta$ approach unity (see $\eta_{\text{new}}$ in Tab. II).

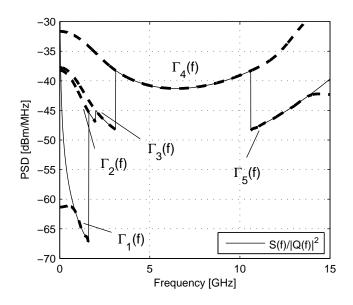The gain in signal power compared to the design of the

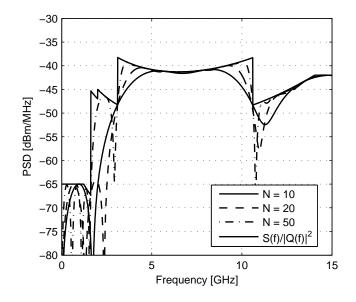Fig. 5. Adapted mask for pulse of $\tau = 0.087$ ns and approximations as $\Gamma_i(f)$ using $I = 5$ intervals



Fig. 7. Optimal design for $\tau = 0.087$ ns after multiplication with pulse PSD



Fig. 6. Optimal design for $\tau = 0.087$ ns

| N | 10 | 20 | 50 |
|---|---|---|---|
| $\eta_{\text{new}}$ $\tau = 0.087$ ns | 0.7135 -1.491 dB | 0.8230 -0.906 dB | 0.9278 -0.325 dB |
| $\eta_{\text{old}}$ $\tau = 0.087$ ns | 0.5350 -2.716 dB | 0.6694 -1.743 dB | 0.7374 -1.323 dB |
| gain due to non-constant bounds | +32.6% 1.225 dB | +21.3% 0.837 dB | +25.8% 0.998 dB |

TABLE II

PERFORMANCE OF OPTIMIZATION WITH NON-CONSTANT PULSE PSD
($\eta_{\text{NEW}}$)

original linear pulseshaping problem is between 22% and 32%, which is between $0.8$ dB and $1.2$ dB. It should be pointed out that this gain does not require any additional resources in implementation. For the same pulse train length $N$, the gain is achieved solely by using better coefficients $w_n$.

### C. The Proposed Design With The Basic Pulse Having $\tau = 0.15$ ns

To give a more drastic example we look into a design where the basic analog pulse cannot be optimally selected: assume the shortest possible pulse is $\tau = 0.15$ ns (see Fig. 1). This leads to much higher performance losses under the constant basic pulse PSD assumption, see $\eta_{\text{old}}$ for $\tau = 0.15$ ns in Tab. III and Fig. 8, since this pulse is far from constant in the important band between 3.1 and 10.6 GHz.
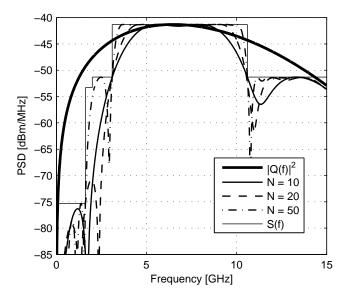
The improved design using the non-constant upper bounds can counter the larger part of these losses (see $\eta_{\text{new}}$ in Tab. III and Fig. 9), but for higher $N$ it approaches unity slowly. As predicted, pulses farther away from the ideal pulse lead to weaker performance, compared to designs using more ideal pulses. This is because pulses farther away from the ideal pulse lead to more challenging FIR filter designs, which in turn will need a higher filter order $N$ to achieve the same results.

Nonetheless, the formulation using non-constant constraints delivers good results, outperforming the old design by about 3 dB.

| N | 10 | 20 | 50 |
|---|---|---|---|
| $\eta_{\text{new}}$ $\tau = 0.15$ ns | 0.5588 -2.527 dB | 0.6518 -1.859 dB | 0.7352 -1.336 dB |
| $\eta_{\text{old}}$ $\tau = 0.15$ ns | 0.2348 -6.293 dB | 0.3205 -4.942 dB | 0.3782 -4.222 dB |
| gain due to non-constant bounds | +138% 3.766 dB | +103% 3.083 dB | +94.4% 2.886 dB |

TABLE III

PERFORMANCE OF OPTIMIZATION WITH DIFFERENT NON-CONSTANT
PULSE PSD ($\eta_{\text{NEW}}$)

these losses. Then we show how the new improved design counters these losses, gaining about 1 dB signal energy in this best-case scenario, which is closest to the constant pulse PSD assumption. Second using a pulse farther from the best-case scenario the losses strongly increase, the improved design shows increased signal energy of about 3 dB.

The gain in both cases is achieved without any extra implementation complexity, since it uses the same filter length $N$. The performance increase is only due to choosing better filter coefficients.

## APPENDIX
## A SIMPLE PROOF OF LEMMA 1

By definition, a square Hermitian matrix $\mathbf{X} \in \mathbb{C}^{N \times N}$ is positive semidefinite iff:

$$\forall \mathbf{y} \in \mathbb{C}^N : \mathbf{y}^H \mathbf{X} \mathbf{y} \geq 0. \tag{29}$$

As a special case we can choose the following $\mathbf{y}$:

$$\mathbf{y} = [1, e^{2\pi Tf}, \ldots, e^{2\pi(N-1)Tf}]$$
$$\Rightarrow \mathbf{y}^H \mathbf{X} \mathbf{y} = \sum_{i=0}^{N-1} \sum_{k=0}^{N-1} [\mathbf{X}]_{i,k} \; e^{j2\pi(k-i)Tf}. \tag{30}$$

When sorting the summation by exponents, we get the left side of (15) using the specified linear relationship between $r_n$ and the elements of $\mathbf{X}$. Hence, the right-hand-side of (15) is a sufficient condition.

To prove necessity, we look at the left side of (15) and state that if $r_n$ satisfies this condition, we can always find a $w_n$, e.g., using spectral factorization [21], leading to

$$\sum_{n=-N+1}^{N-1} r_n e^{j2\pi nTf} = \left| \sum_{n=0}^{N-1} w_n e^{j2\pi nTf} \right|^2$$
$$= \left| \mathbf{w}^H \mathbf{y} \right|^2 \tag{31}$$
$$= \mathbf{y}^H \left( \mathbf{w}\mathbf{w}^H \right) \mathbf{y}$$

using the definition of $\mathbf{y}$ from (30) and $\mathbf{w} = [w_o, \ldots, w_{N-1}]^H$. This immediately proves (15) is a necessary condition, since we have shown that there exists at least one satisfactory $\mathbf{X}$: $\mathbf{w}\mathbf{w}^H$ a positive semidefinite matrix with diagonals that sum to $\sum_{k=0}^{N-1-n} w_k w_{k+n} = r_n$. $\square$

## REFERENCES

[1] K. Siwiak and D. McKeown, *Ultra-Wideband Radio Technology*. John Wiley & Sons, 2004.
[2] M. Ghavami, L. B. Michael, and R. Kohno, *Ultra Wideband Signals and Systems in Communication Engineering*. John Wiley & Sons, 2004.
[3] M. G. Di Benedetto and G. Giancola, *Understanding Ultra Wide Band Radio Fundamentals*. Prentice Hall PTR, 2004.
[4] S. Stroh, "Ultra-wideband: Multimedia unplugged," *IEEE Spectrum*, vol. 40, no. 9, pp. 23–27, Sept. 2003.
[5] Federal Communications Commission, "In the matter of revision of part 15 of the commission's rules regarding ultra-wideband transmission systems, First Report and Order," Apr. 2002.
[6] J. H. McClellan and T. W. Parks, "A unified approach to the design of optimum FIR linear-phase digital filters," *IEEE Trans. Circuit and Systems*, vol. 20, no. 6, pp. 697–701, Nov. 1973.
[7] X. Luo, L. Yang, and G. B. Giannakis, "Designing optimal pulse-shapers for UWB radios," *Journal of Communications and Networks*, vol. 5, no. 4, pp. 344–353, Dec. 2003.
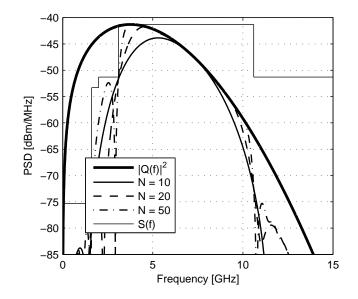
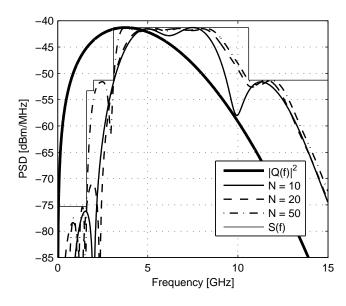Fig. 8. Losses due to non-ideal pulse of $\tau = 0.15$ ns



Fig. 9. Optimal design for $\tau = 0.15$ ns

## V. CONCLUSION

We have presented an implementation of semidefinite programming based FIR filter design with non-constant constraints. To this end we took a closer look at existing linear matrix inequality formulation used for FIR filter design via semidefinite programming and chose an implementation accommodating non-constant bounding functions. We can approximate any piece-wise continuous bounding function via a modified Fourier series expansion using non-orthogonal basis functions.

This implementation leads to an improved UWB pulse-shaper design, rendering the assumption of a constant basic analog pulse PSD unnecessary.

In our detailed design examples, we first analyze the loss in performance incurred when using a real analog pulse, i.e., the Gaussian Monocycle, which we first chose to minimize

[8] S.-P. Wu, S. Boyd, and L. Vandenberghe, "FIR filter design via semidefinite programming and spectral factorization," in *Proceedings of the 35th Conference on Decision and Control*, vol. 1. IEEE, Dec. 1996, pp. 271–276.

[9] T. N. Davidson, Z.-Q. Luo, and J. F. Sturm, "Linear matrix inequality formulation of spectral mask constraints with applications to FIR filter design," *IEEE Trans. Signal Processing*, vol. 50, no. 11, pp. 2702–2715, Nov. 2002.

[10] S. Boyd and L. Vandenberghe, *Convex Optimization*. Cambridge, U.K.: Cambridge University Press, 2004.

[11] X. Wu, Z. Tian, T. N. Davidson, and G. B. Giannakis, "Optimal waveform design for UWB radios," *IEEE Trans. Signal Processing*, vol. 54, no. 6, pp. 2009–2021, June 2006.

[12] L. Yang and G. B. Giannakis, "Ultra-wideband communications: An idea whose time has come," *IEEE Trans. Signal Processing*, vol. 21, no. 6, pp. 26–54, Nov. 2004.

[13] J. G. Proakis, *Digital Communications*, 4th ed. New York: McGraw-Hill, 2001.

[14] M. Z. Win, "Spectral density of random UWB signals," *IEEE Commun. Lett.*, vol. 6, no. 12, pp. 526–528, Dec. 2002.

[15] ——, "A unified spectral analysis of generalized time-hopping spread-spectrum signals in the presence of timing jitter," *IEEE J. Select. Areas Commun.*, vol. 20, no. 9, pp. 1664–1676, Dec. 2002.

[16] B. Parr, B. L. Cho, K. Wallace, and Z. Ding, "A novel ultra-wideband pulse design algorithm," *IEEE Commun. Lett.*, vol. 7, no. 5, pp. 219–221, May 2003.

[17] L. Vandenberghe and S. Boyd, "Semidefinite programming," *SIAM Review*, vol. 31, no. 1, pp. 49–95, Mar. 1996.

[18] J. F. Sturm, "Using SeDuMi 1.02, a MATLAB toolbox for optimization over symmetric cones," *Optimization Methods and Software*, vol. 11-12, pp. 625–653, 1999.

[19] T. N. Davidson and J. F. Sturm, "A primal positive real lemma for FIR systems, with application to filter design and spectral factorization," Communications Research Laboratory, McMaster University, Hamilton, Canada, Technical report, Feb. 2000.

[20] T. N. Davidson, Z.-Q. Luo, and K. M. Wong, "Design of orthogonal pulse shapes for communications via semidefinite programming," *IEEE Trans. Signal Processing*, vol. 48, no. 5, pp. 1433–1445, May 2000.

[21] B. D. Anderson and K. L. Hitz, "Recursive algorithm for spectral factorization," *IEEE Trans. on Circuits and Systems*, vol. 21, no. 6, pp. 742–750, Nov. 1974.

PLACE PHOTO HERE

**Michael Eisenacher** received the Dipl.-Ing. from the Technical University of Darmstadt, Germany in 2002 and the Ph.D. degree from the the Universität Karlsruhe (TH), Germany in 2006 both in electrical engineering.

He is currently with Continental Automotive Systems, Lindau, Germany, working on the development of automotive radar sensors. His research interests are signal processing for UWB systems and radar sensors. He was involved in the miniWatt project, funded by the German Ministry of Research and Technology, and the integrated research project PULSERS (Pervasive Ultra-Wideband Low Spectral Energy Radio Systems), funded by the European Union IST programme. Mr. Eisenacher is an author of several conference and journal papers.

PLACE PHOTO HERE

**Shengli Zhou** (M'03) received the B.S. degree in 1995 and the M.Sc. degree in 1998, from the University of Science and Technology of China (USTC), Hefei, both in electrical engineering and information science. He received his Ph.D. degree in electrical engineering from the University of Minnesota (UMN), Minneapolis, in 2002. He has been an assistant professor with the Department of Electrical and Computer Engineering at the University of Connecticut (UCONN), Storrs, since 2003.

His research interests lie in the areas of communications and signal processing, including multi-user and multi-carrier communications, communications with feedback, wireless positioning and synchronization, underwater acoustic communications and networking, and cross-layer designs. He has served as an associate editor for IEEE Transactions on Wireless Communications since 2005.

PLACE PHOTO HERE

**Prof. Dr. rer.nat. Friedrich K. Jondral** received a Diploma in mathematics and a Doctoral degree in natural sciences from the Technische Universität Braunschweig, Germany, in 1975 and 1979, respectively. During the winter semester 1977/78 he was a visiting researcher to the Department of Mathematics, Nagoya University, Japan. From 1979 to 1992 Dr. Jondral was an employee of AEGTelefunken (now European Aeronautic Defence and Space Company, EADS), Ulm, Germany, where he held various research, development and management positions. Since 1993 Dr. Jondral has been Full Professor and Head of the Institut für Nachrichtentechnik at the Universität Karlsruhe (TH), Germany. Here, from 2000 to 2002, he served as the Dean of the Department of Electrical Engineering and Information Technology. During a sabbatical in the summer semester 2004, Dr. Jondral was a visiting faculty to the Mobile and Portable Radio Research Group of Virginia Tech, Blacksburg, VA. His current research interests are in the fields of ultra wideband communications, software defined and cognitive radio, signal analysis, pattern recognition, network capacity optimization and dynamic channel allocation.

PLACE PHOTO HERE

**Christian R. Berger** (S'05) received the Dipl.-Ing. in electrical engineering in 2005, from the Universität Karlsruhe (TH), Germany. During this degree he also spent a semester at the National University of Singapore (NUS), where he took both undergraduate and graduate courses in electrical engineering. He is currently pursuing the Ph.D. degree in electrical engineering at the University of Connecticut (UCONN), Storrs.

His research interests lie in the areas of communications and signal processing, including distributed estimation in wireless sensor networks, wireless positioning and synchronization, underwater acoustic communications and networking.